ACS APPLIED MATERIALS & INTERFACES

Forum Article

www.acsami.org

Stretch-Induced Helical Conformations in Poly(L-lysine)/Hyaluronic Acid Multilayers

Sarah Zahouani,[†,‡] Alain Chaumont,[§] Bernard Senger,[†,‡] Fouzia Boulmedais,[∥,⊥] Pierre Schaaf,*[,†,‡,∥,⊥] Loïc Jierry,[∥,⊥] and Philippe Lavalle*[,†,‡]

[†]Institut National de la Santé et de la Recherche Médicale, INSERM Unité 1121, 11 rue Humann, 67085 Strasbourg Cedex, France

[‡]Faculté de Chirurgie Dentaire, Université de Strasbourg, 8 rue Sainte Elisabeth, 67000 Strasbourg, France

[§]Faculté de Chimie, UMR 7177, Université de Strasbourg, 1 rue Blaise Pascal, 67008 Strasbourg Cedex, France

[∥]Institut Charles Sadron, CNRS UPR 22, 23 rue du Lœss, 67034 Strasbourg Cedex, France

[⊥]University of Strasbourg Institute of Advanced Study, 5 allée du Général Rouvillois, 67083 Strasbourg Cedex, France

Supporting Information

ABSTRACT: We investigate the effect of stretching on the secondary structure of cross-linked poly(L-lysine)/hyaluronic acid (PLL/HA) multilayers. We show that stretching these films induces changes in the secondary structure of PLL chains. Our results suggest that not only α- but also 3_{10}-helices might form in the film under stretching. Such 3_{10}-helices have never been observed for PLL so far. These changes of the secondary structure of PLL are reversible, i.e., when returning to the nonstretched state one recovers the initial film structure. Using molecular dynamics simulations of chains composed of 20 L-lysine residues (PLL20), we find that these chains never adopt a helical conformation in water. In contrast, when the end-to-end distance of the chains is restrained to values smaller than the mean end-to-end distance of free chains, a distance domain rarely explored by the free chains, helical conformations become accessible. Moreover, the formation of not only α- but also 3_{10}-helices is predicted by the simulations. These results suggest that the change of the end-to-end distance of PLL chains in the stretched film is at the origin of the helix formation.

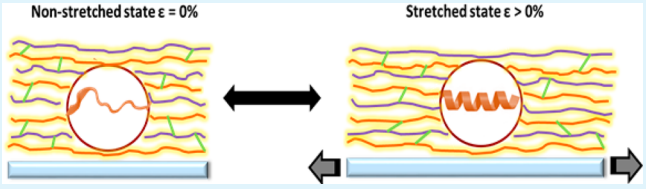

KEYWORDS: *polyelectrolyte multilayers, mechanoresponsive materials, circular dichroism, molecular dynamics, secondary structure*

INTRODUCTION

The role of mechanical forces in biological processes and their interplay with chemistry have emerged recently as an important issue and constitute now a major field of research. Cells, for example, sense continuously the mechanical properties of their environment.[1,2] The mechanisms involved consist of applying forces onto their surrounding extracellular matrix or onto their neighboring cells. These forces are then transduced into chemical responses through various physicochemical processes, one of them being based on stretch-induced protein conformational changes.[3] Such a strategy has inspired our group, leading us to design original materials that transduce a mechanical signal into a chemical response.[4,5] This new branch in the field of mechanochemistry based on conformational changes can be called "Soft-Mechanochemistry". In contrast with the current mechanochemical developments based on modifying chemical bonds by stretching forces,[6] soft-mechanochemistry is based on mechanically induced chemical processes relying on conformational changes of macromolecules or of macromolecular films. Because conformational changes are usually in the 1−10 kcal mol^{-1} range compared to 50−100 $kcal.mol^{-1}$ for covalent bonds,[7] the energies required in soft-mechanochemistry to induce chemical processes are by far much smaller than what is required in "conventional" mechanochemistry. Moreover, one can expect that the processes onto which soft-mechanochemistry is based are at least partially reversible. There already exist several examples of soft-mechanochemistry processes such as the stretch-induced modulation of enzymatic reactions[4,5] or the reversible tuning of the torsion angle of amphiphilic chiral molecules at the air/water interface by application of a mechanical force at a molecular monolayer.[8]

According to several theoretical predictions, a coil-to-helix transition can be induced by stretching macromolecules which are close to the spontaneous coil-to-helix transition. This transition appears to be driven by enthalpy with a loss of entropy.[9−12] Such helical transition induced by a mechanical stress was demonstrated experimentally by AFM force spectroscopy on DNA[13] and by Courty et al. on a gelatin network.[14] These authors showed that optical rotation increases with deformation of the gelatin network due to the transition of denatured chains to the natural left-handed helical state. To the best of our knowledge, this is the only reported macroscopic system where stretching induces helical structures.

Special Issue: Current Trends in Functional Surfaces and Interfaces for Biomedical Applications

Received: September 4, 2015
Accepted: November 24, 2015
Published: December 8, 2015

DOI: 10.1021/acsami.5b08302
ACS Appl. Mater. Interfaces 2016, 8, 14958−14965

Scheme 1. Schematic Representation of the Cross-Linked Multilayer Film (PLL/HA) Adsorbed onto a PDMS (poly(dimethyl siloxane) Substrate[a]

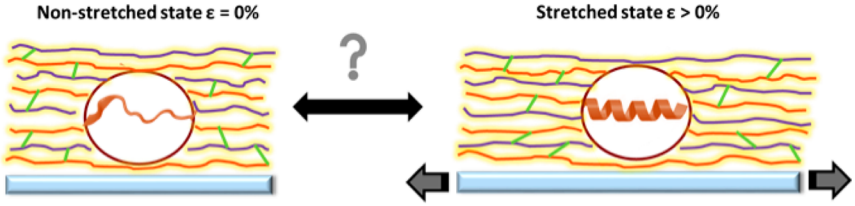

[a]The longitudinal stretching of the (PLL/HA)@PDMS material leads to a mechanical stress imposed to both polymers, PLL and HA. Their conformational behaviors are monitored through CD measurements.

Polyelectrolyte multilayer (PEM) films represent an ideal tool to functionalize surfaces.[15−20] These films are obtained by the alternate deposition of polyanions and polycations on a solid substrate.[21] They are based on electrostatic interactions between the polyanions and the polycations and can be easily prepared on all kind of substrates with a large variety of polyanion/polycation pairs. Among these polyelectrolytes, poly(amino acids) are well suited when focusing on biocompatible coatings. In this context, poly(L-lysine) (PLL) has been widely used.[22] PLL is a cationic poly(amino acid) known to undergo a reversible transition of conformation between random coil and helix when the pH changes.[23,24] Polyelectrolyte multilayers containing PLL thus appear at first sight as promising candidates for studying systems undergoing a stretch-induced coil-to-helix transition. The goal of this article is to address this issue (Scheme 1). This experimental study will be complemented by molecular dynamics simulations in order to gain some insight into the experimental results.

For these experiments, we will use multilayers built with PLL and hyaluronic acid (HA), which can reach thicknesses of several micrometers after 20 deposition steps. They behave as a viscous liquid,[25−27] but chemical cross-linking between PLL and HA chains allows for providing elastic and nonbreakable films.[5] As main experimental tool, we will use circular dichroism to follow the secondary structure of the multilayer.

EXPERIMENTAL SECTION

Materials. Poly(L-lysine) hydrobromide (PLL, Mw = 52 000) was purchased from Alamanda Polymers (Huntsville, USA) and hyaluronic acid (HA, Mw = 132 000) from Lifecore Biomedical (Chaska, USA). Poly(ethylenimine) (PEI, Mw = 750 000), poly(L-lysine)-fluorescein isothiocyanate (PLL-FITC) (Mw = 15 000−30 000), tris-(hydroxymethyl)aminomethane (Tris), sodium chloride (NaCl), and the coupling agents N-(3-(dimethylamino)propyl)-N′-ethylcarbodiimide hydrochloride (EDC, ≥ 98%) and *N*-hydroxysulfosuccinimide sodium salt (sulfo-NHS, ≥ 98%) were obtained from Sigma-Aldrich (Saint-Quentin Fallavier, France). Poly(dimethylsiloxane) (PDMS) sheets of 254 μm thickness (Specialty Manufacturing Inc., Saginaw, USA) were chosen as substrates for the construction of PEM films.

Buildup of PEM Films. PEM films were built with an automated dipping robot (Riegler & Kirstein GmbH, Berlin, Germany) on the silicone sheets. They were previously cleaned with ethanol and then extensively rinsed with water. The polyelectrolytes used for the construction of the multilayers were dissolved in a 0.15 M NaCl solution prepared with deionized water (22.5 μS) and used at a concentration of 1 mg.mL^{-1}. Silicone substrates were first dipped in the PEI solution (polycation) for 4 min followed by two rinsing steps of 5 min each in a NaCl (0.15 M) solution. This first step was performed in order to form an anchoring layer on the silicone substrates. The PLL/HA architecture was then obtained by dipping the silicone substrates in a HA solution (polyanion) for 4 min followed by two rinsing steps of 5 min each in the NaCl (0.15M) solution. The PLL polycations were then deposited in the same manner. The buildup process was pursued by the alternated deposition of HA and PLL. In this study, the actual formulation of the films is PEI/HA/$(PLL/HA)_{23}$, but for the sake of simplicity the $(PLL/HA)_n$ notation (with n = 23) will be used in the manuscript.

Cross-Linking of the PLL/HA Films by EDC-Sulfo-NHS. Cross-linking was performed by immersing the PEM films in a solution containing EDC (20 mM) and Sulfo-NHS (50 mM) in NaCl (0.15 M) during 15 h at 4 °C. At the end of this step, the films were rinsed 4 times with a NaCl (0.15 M) solution. Then a buffer solution (NaCl 0.15 M/Tris 10 mM, pH 7.4) was used for the last rinsing step. The films were stored in this buffer at 4 °C.

Stretching Device. The homemade stretching device used for the experiments was composed of two jaws made of stainless steel allowing to tighten the films and to stretch them manually in a uniaxial direction.[5] The stretching rate (or strain) ε has been defined by the relation $\varepsilon = 100 \times (L - L_0)/L_0$ (in %) where L_0 and L represent respectively the lengths in the nonstretched and in the stretched states. The experiments were performed at room temperature in the presence of buffer solution (NaCl 0.15 M/Tris 10 mM, pH 7.4) to avoid the drying of the films.

Circular Dichroism. Circular dichroism (CD) spectra were recorded using a Jasco J-810 spectropolarimeter with a data pitch of 1 nm on the light wavelength. CD spectra are obtained by shining the polarized light beam perpendicularly through the silicone sheet covered by the PLL/HA film. The CD spectra show the ellipticity expressed as an angle as a function of the wavelength. Liquid samples were inserted in a quartz cell of path length 1 mm. Solutions were maintained at adequate temperatures using a Peltier apparatus (Jasco-PTC-423S) with an accuracy of ±0.2 °C. Nonstretched and stretched PEM films were stored in the buffer solution (NaCl 0.15M/Tris 10 mM, pH 7.4) between two measurements and great care was taken to maintain them in a hydrated state.

Confocal Laser Scanning Microscopy. Observations were carried out with a Zeiss LSM 710 microscope (Heidelberg, Germany) using a 20× objective (Zeiss, Plan Apochromat). Before performing the measurements, non-cross-linked and cross-linked $(PLL/HA)_{23}$ films were loaded with PLL-FITC to visualize the thickness and homogeneity of the polyelectrolytes within the multilayers. To this end, 100 μL of a PLL-FITC solution at a concentration of 0.5 mg.mL^{-1} (in a NaCl 0.15 M solution) were deposited on top of PEM films incubated for 10 min before rinsing two times with 200 μL of NaCl 0.15 M solution for 10 min each. The films were then placed into the stretching device, hydrated with the buffer solution and observed in the nonstretched state and in a stretched state (ε = 80%). FITC fluorescence was detected after excitation at λ = 488 nm with an argon laser and a cutoff dichroic mirror of 488 nm and an emission band-pass filter of 505−530 nm (green emission). The mobility of polyelectrolyte chains within the films was qualitatively determined by photobleaching experiments (FRAP, Fluorescence Recovery After Photobleaching).[28] A circular region of interest (10.6 μm in radius) in the image (256 × 256 pixels, 84.9 μm × 84.9 μm) was bleached with the laser set at its maximum power. Then, the recovery of the fluorescence in the bleached area was observed at different postbleach

DOI: 10.1021/acsami.5b08302
ACS Appl. Mater. Interfaces 2016, 8, 14958−14965

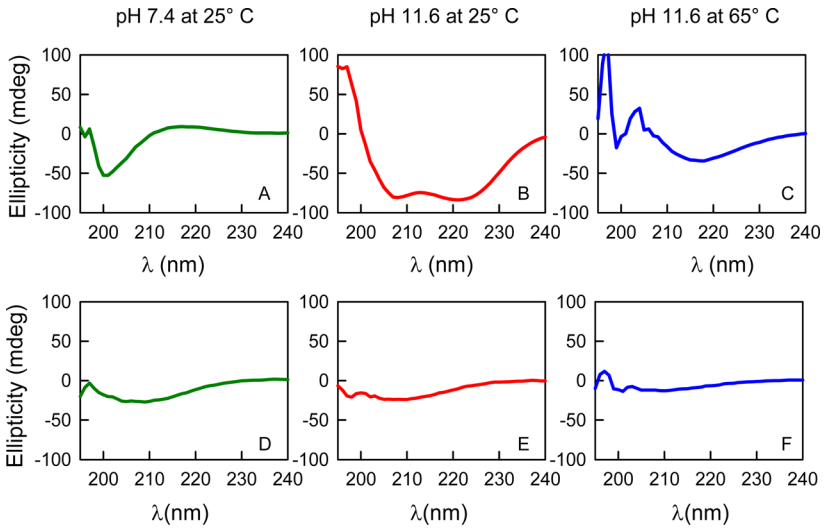

Figure 1. CD spectra of PLL (52 000 Da) solution (0.5 mg.mL^{-1}) in NaCl (0.15 M) at different pH and temperatures: (A) pH 7.4 at 25 °C, (B) pH 11.6 at 25 °C, and (C) pH 11.6 at 65 °C. CD spectra of HA (132 000 Da) solution (0.5 mg mL^{-1}) in NaCl (0.15 M) at different pH and temperatures: (D) pH 7.4 at 25 °C, (E) pH 11.6 at 25 °C, and (F) pH 11.6 at 65 °C.

times ranging from 0.7 s up to 150 s. The images were analyzed by means with the "ImageJ" software.[29]

Molecular Dynamics (MD) Simulations. The systems were simulated by classical molecular dynamics (MD) using the AMBER.14 GPU software[30] in which the potential energy U is empirically described by a sum of bond, angle and dihedral deformation energies and pairwise additive 1−6−12 (electrostatic + van der Waals) interactions between nonbonded atoms.

$$U = \sum_{\text{bonds}} k_b(r - r_0)^2 + \sum_{\text{angles}} k_\theta(\theta - \theta_0)^2 + \sum_{\text{dihedrals}} \sum_{n} V_n(1 + \cos(n\varphi - \gamma)) + \sum_{i<j} \left[\frac{q_i q_j}{R_{ij}} - 2\varepsilon_{ij}\left(\frac{R_{ij}^*}{R_{ij}}\right)^6 + \varepsilon_{ij}\left(\frac{R_{ij}^*}{R_{ij}}\right)^{12} \right]$$

Bond and angle deformations are represented using a harmonic potential with force constants k_b and k_θ, respectively, and either an equilibrium distance r_0 or an equilibrium angle θ_0. The dihedral deformation energy is described using a torsional potential where V_n is the barrier height divided by 2, n the periodicity of the torsional barrier and γ the phase shift angle of the torsional function. Pairwise electrostatic interactions are obtained via Coulomb's law where q_i and q_j are the atomic charges centered on atom i and j, respectively, whereas R_{ij} is the distance between these atoms. van der Waals interactions are calculated using a pairwise 6−12 Lennard-Jones potential where R_{ij}* corresponds to the distance at which this potential reaches its minimum.

The simulated systems are composed of a 20-residue poly(L-lysine) chain (PLL20) and about 7500 water molecules. 20% of the PLL20 side chains were deprotonated; additionally the system was neutralized by adding 16 Cl^- ions. Force-field parameters for the PLL20 were taken from the AMBER ff14SB force field which has been optimized to improve the accuracy of protein side-chains and backbone parameters compared to previous AMBER force-fields,[31,32] whereas those for Cl^- are taken from the work of Cheatham et al.[33,34] The TIP3P model was used for water.[35] Cross terms in van der Waals interactions were constructed using the Lorentz−Berthelot rules. 1−4 van der Waals and 1−4 electrostatic interactions were scaled by a factor of 2. The MD simulations were performed at 300 K starting with random velocities. The temperature was monitored by coupling the system to a thermal bath using the Berendsen algorithm with a relaxation time of 1 ps. A time step of 2 fs was used to integrate the equations of motion via the Verlet leapfrog algorithm. Some simulations were performed restraining the end-to-end distance between both terminal Cα atoms of the PLL20. The values of the end-to-end distance to which the system was restrained ranges from 2 to 4 nm by steps of 0.4 nm. The restraint was applied using a parabolic potential with a force constant k of 1 × 10^4 kcal mol^{-1} nm^{-2}. The trajectories were analyzed using the cpptraj software.[36] Snapshots along the trajectory were taken using the VMD software.[37]

RESULTS AND DISCUSSION

Poly(L-lysine) is a polypeptide whose secondary structures in aqueous solution are known to vary with pH. As previously specified, under acidic and neutral conditions PLL adopts a random coil conformation and undergoes a coil-to-helix transition under basic conditions. At pH 11.6, it is fully in an α-helix conformation.[23,24] The spectra of PLL solutions at pH 7.4 and pH 11.6 at room temperature were used as references of Circular Dichroism (CD) spectra of PLL in the random coil and α-helix conformations, respectively (Figure 1). A unique negative minimum at 202 nm is observable at pH 7.4 and is characteristic of a random coil conformation (Figure 1A). One can also mention the left-handed trans PolyProline II (P_{II}) conformation, which is rather observed for PLL at low temperatures,[38] distinguished by the absence of internal hydrogen bonding and with a spectrum characterized by a strong negative minimum at 195 nm and a shallow positive maximum near 213 nm.[39] In our case, the negative minimum rather appears at 202 nm, which is characteristic of a random coil conformation as suggested above. Thus, the P_{II} structure was ignored in our interpretations even if one cannot fully exclude a contribution of it. The α-helix conformation obtained at pH 11.6 is easily recognizable by a positive band at about 195 nm and two negative minima centered, in solution, at 210 and 222 nm (Figure 1B). As described in the literature, PLL in aqueous solution at pH 11.6 and heated to 65 °C exhibits a spectrum corresponding to a β-sheet conformation with a positive maximum at about 202 nm and a broad negative minimum at 217 nm (Figure 1C).[23,24,40,41] We also determined the CD spectra of the polyanion (HA), at pH 7.4 at room temperature (Figure 1D), at pH 11.6 at room temperature (Figure 1E) and at pH 11.6 at 65 °C (Figure 1F). No

DOI: 10.1021/acsami.5b08302
ACS Appl. Mater. Interfaces 2016, 8, 14958−14965

significant changes are observed between these conditions and all the spectra correspond to unordered conformations of HA chains.

Then, we built $(PLL/HA)_{23}$ multilayer films onto silicone substrates. Because PLL/HA films behave as a viscous liquid, we cross-linked them through EDC-NHS chemistry.[19] This cross-link step is intended to allow the transmission of the forces generated by stretching the silicone sheet to the PLL and HA chains constituting the film without inducing crack formation.[5] Using FRAP experiments on films containing PLL-FITC, we observe that the recovery of fluorescence in the bleached area is significant after 150 s in the case of a non-cross-linked film whereas no recovery of fluorescence is observed in the cross-linked film (Figure S1A, B). This indicates that all PLL-FITC chains and most probably all PLL chains are cross-linked within the PLL/HA matrix. As a consequence, most of the PLL chains in the film should be affected by stretching.

Non-cross-linked and cross-linked films stored in a buffer solution (NaCl 0.15 M/Tris 10 mM, pH 7.4) at room temperature were also compared by CD analysis in the nonstretched state in order to check the influence of cross-link on the chain conformations. Typical CD spectra of nonstretched PLL/HA films are given in Figure S2 and we can observe that cross-linking the film does not affect its CD spectrum. Indeed, the spectra of nonstretched PLL/HA films, cross-linked or not, are close to the spectrum of PLL in solution at pH 7.4 which corresponds to a random coil conformation with a minimum centered at 202 nm. There is no sign of the presence of two negative minima at 210 and 222 nm, indicating that the polyelectrolyte chains do not adopt any helix conformation. There is also no sign of a β-sheet structure because of the absence of a minimum at 217 nm. In summary, it appears that cross-linking does not affect the secondary structure of the films and is expected to allow transmission of mechanical forces to the chains. Therefore, we used only cross-linked films in the following.

Next, knowing that PLL adopts an α-helix conformation as unique folding at pH 11.6 in solution, some cross-linked $(PLL/HA)_{23}$ films built onto PDMS at pH 7.4 were immersed into a basic solution (NaCl 0.15 M/Tris 10 mM, pH 11.6) at room temperature for 2 h. CD measurements in the nonstretched state were carried out to observe the helicity of PLL chains inside the films. Interestingly, the resulting spectrum (Figure 2) is different from the typical one measured with pure PLL in solution at pH 11.6 (Figure 1). As displayed in Figure S6a, we could never obtain a good fit of this spectrum by a linear combination of the spectra relative to HA and the different secondary structures of PLL observed in solution (whereas combining the random coil conformation of PLL in solution at pH 7.4 with the conformation of HA fits well with the CD spectrum of a nonstretched, cross-linked PLL/HA film at pH 7.4 (Figure S6b)). The spectrum relative to a cross-linked PLL/HA film at pH 11.6 is rather close to the spectrum relative to another helical conformation well-known in proteins and called 3_{10}-helix. Actually, the two minima at 210 and 222 nm have the same intensity in the case of the α-helix whereas the minimum at 222 nm is less intense for the 3_{10}-helix.[42] This right-handed helical structure is the third principal structure occurring in globular proteins and is more tightly bound than the α-helix.[43,44] Indeed, the intramolecular C═O···H−N hydrogen bonding schemes are significantly different in the two helices, being of the $i+3 \rightarrow i$ type with 10 atoms in the ring in the 3_{10}-helix (the amino group of residue $i+3$ forms a hydrogen bond with the carbonyl group of residue i), whereas it is of the $i+4 \rightarrow i$ type with 13 atoms in the ring in the α-helix. This observation indicates that the helicity of PLL at pH 11.6 is different in the cross-linked film than in solution. This may be due to the presence of HA chains in the film that may influence the resulting CD spectra of PLL. Another possibility might be that cross-linking induces constraints that may also influence helicity of PLL chains (see further discussion in Simulation section).

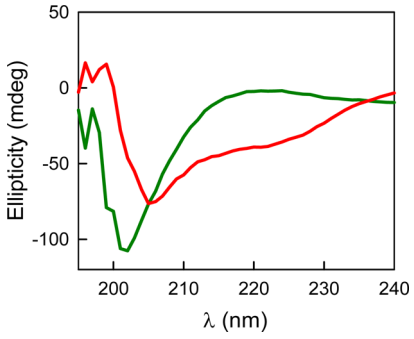

Figure 2. CD spectra of a cross-linked $(PLL/HA)_{23}$ film in the nonstretched state (ε = 0%) at pH 7.4 (green) and pH 11.6 (red).

The cross-linked PLL/HA films were then stretched at various degrees ranging from ε = 20% up to ε = 80%. It must be noticed that each spectrum was taken from a freshly prepared film. The spectra were monitored about 10 min after stretching but no changes were noticed when keeping the films in the stretched state for 24 h showing that the PLL chains reach very quickly a stable structure after stretching. For the strains of 20 and 40%, two types of behavior were observed. At ε = 20%, we observe spectra (Figure 3B) close to those of nonstretched films even if the minimum shifts slightly toward higher wavelengths (typically 204−206 instead of 202 nm). There are other films stretched at 20% with spectra clearly different from the nonstretched ones (Figure 3C), showing two minima, one centered at about 209 nm and a second, weaker minimum centered between 220 and 225 nm. When stretching the films to ε = 40%, the two behaviors continue to be observed (Figure 3D, E) but for the films presenting spectra with two minima, the intensity of the second minimum at 220−225 nm becomes shallower and transforms into a shoulder (Figure 3E). From a qualitative point of view we can assume that the spectra of films with two minima centered at 209 and 220−225 nm correspond to the formation of helices under mild stretching. When reaching strains of ε = 60% (Figure 3F) and ε = 80% (Figure 3G) only a single group of spectra is observed for both values of ε showing a single minimum band centered at about 207 nm and a shoulder located at about 220−225 nm. These spectra closely resemble those corresponding to nonstretched cross-linked films at pH 11.6 that are similar to spectra of 3_{10}-helices. This seems to indicate that stretching a film at pH 7.4 above ε = 60% induces structural changes which can eventually be attributed to 3_{10}-helices. The bivalent behavior of the films at 20 and 40% stretching might come from the fact that at low stretching degrees the system is very sensitive to different parameters such as the temperature or the degree of humidity in the experimental device during CD measurement or the precise stretching rate that cannot be controlled with a high degree of accuracy due to technical difficulties. Above 40%, the

DOI: 10.1021/acsami.5b08302
ACS Appl. Mater. Interfaces 2016, 8, 14958−14965

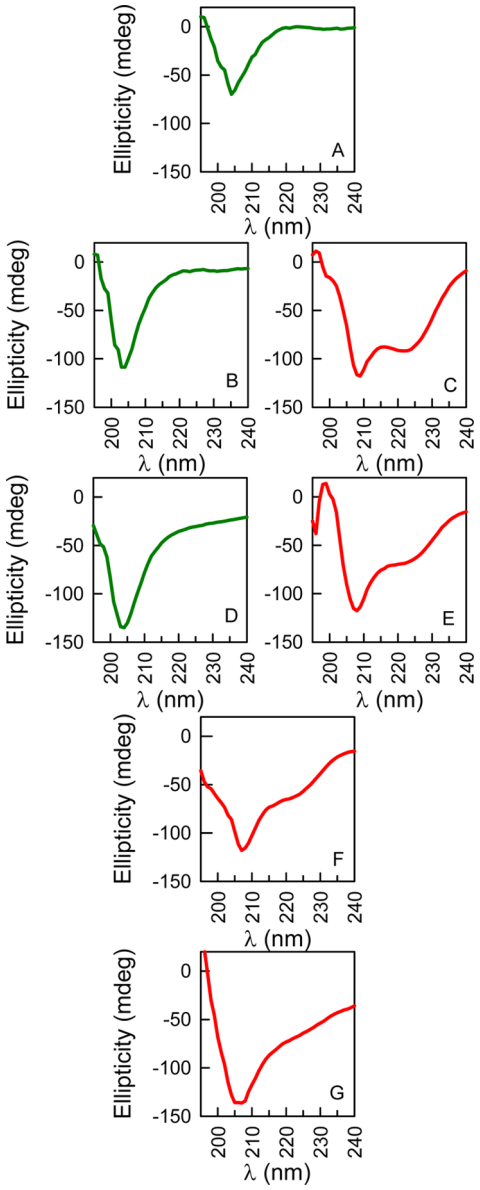

Figure 3. Representative CD spectra of $(PLL/HA)_{23}$ films for different strain values: ε = (A) 0,(B, C) 20,(D, E) 40, (F) 60, and (G) 80%.

stretching is always sufficient to ensure structural transition of PLL.

To further highlight the evolution of PLL conformation into the cross-linked $(PLL/HA)_{23}$ films observed in CD spectra shown in Figure 3, we analyzed all these spectra in the wavelength bracket 200−240 nm, where shape changes are expected if a transition from the random coil conformation to helices occurs. To this end, we determined the moments of first, second, and third order of λ from which we derived the average and the skewness (for details, see Supporting Information). Figure 4 shows the skewness, γ_1, of the spectrum as a function of the weighted average of λ, $\langle\lambda\rangle$, within the above-mentioned interval for all spectra that have been recorded in the present study. As can be observed, the representative data points tend to follow a unique curve. Nonstretched systems correspond to small values of $\langle\lambda\rangle$ and γ_1 ranging from 1.5 to 2.5. For a given strain, the data points group into domains distributed along this curve in a fairly regular manner: as the strain increases, $<\lambda>$ increses and γ_1

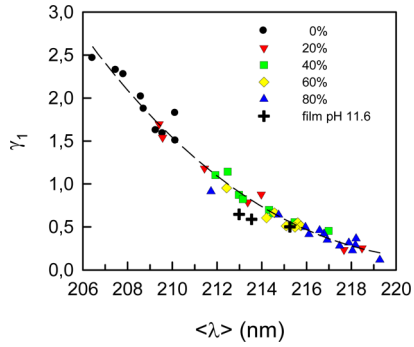

Figure 4. Skewness of the CD spectra as a function of the weighted average of the wavelength within the domain 200−240 nm. Several spectra are available for a given strain ε: 0% (black dots), 20% (red triangles down), 40% (green squares), 60% (yellow diamonds), and 80% (blue triangles up). The dashed line serves merely to guide the eye. Three nonstretched $(PLL/HA)_{23}$ films at pH 11.6 are represented by black crosses.

decreases. This indicates a continuous evolution of the film secondary structure with strain. However, it should also be observed that for low strain, the data points are scattered over large $\langle\lambda\rangle$ and γ_1 domains which shows that there is a high variability in the secondary structure of these films as already suggested above in the comment to Figures 3B, C. It is also worth noting that the data points, corresponding to non-stretched films at pH 11.6 where PLL is known to adopt an helical conformation, fall into the high-strain region of the films at pH 7.4 (Figure 4).

After having demonstrated that stretching induces structural changes, expected to be the formation of helices in $(PLL/HA)_{23}$ films, the reversibility of the structural change will now be addressed. Cross-linked $(PLL/HA)_{23}$ films prepared in buffer solution (NaCl 0.15 M/Tris 10 mM, pH 7.4) were kept stretched at ε = 20, 40, 60 or 80% during 10 min. Then, all films were brought back to ε = 0% and spectra were recorded 20 min later. Figure 5 shows a typical example corresponding to

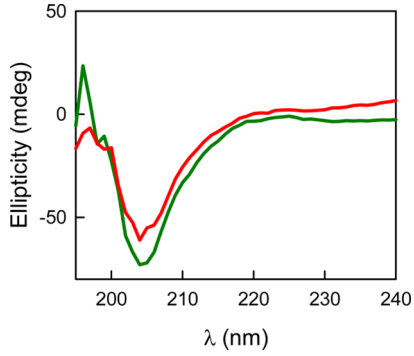

Figure 5. CD spectra of a cross-linked $(PLL/HA)_{23}$ film in the nonstretched state (ε = 0%) (green) and brought back to the nonstretched state after stretching at ε = 80% (red).

a film brought back to the nonstretched state after stretching at 80%. The spectrum clearly indicates that the films recover their initial structure with a unique minimum at about 202 nm corresponding to a random coil conformation of the PLL. The same observation was done for films stretched at ε = 20, 40, and 60%, and brought back to ε = 0% (Figure S3). The stretch-induced structural transition of the cross-linked PLL/HA films appears thus fully reversible in a few minutes.

DOI: 10.1021/acsami.5b08302
ACS Appl. Mater. Interfaces 2016, 8, 14958−14965

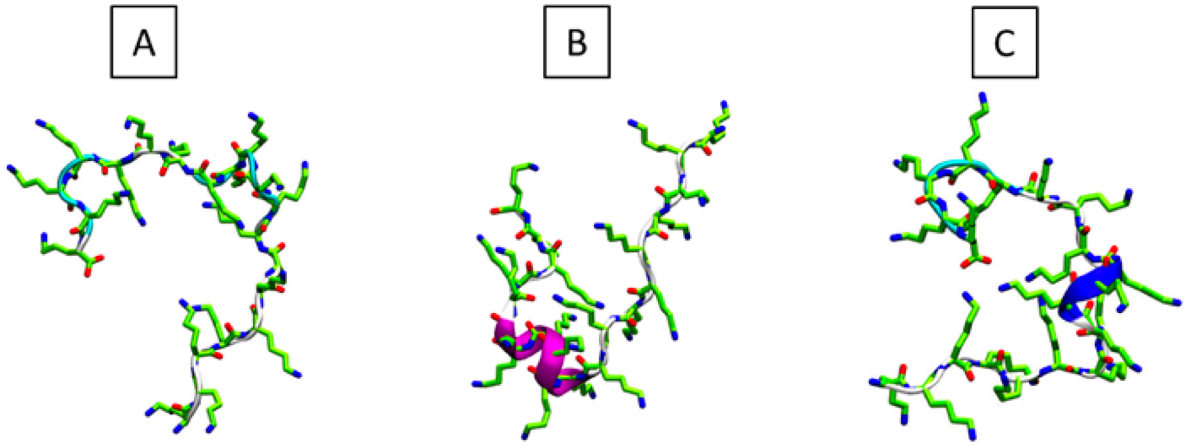

Figure 6. Snapshots of conformations along PLL20: (A) coil conformation, (B) α-helix (purple strand), and (C) 3_{10}-helix (blue strand section).

To gain more insight into these experimental results, we performed a molecular dynamics (MD) study. In particular, our goal was to relate the evolution of the conformational behavior of PLL as a function of the end-to-end distance of the polymer chain. Experimentally, stretching the material should change the end-to-end distance distribution of the PLL chains. In particular, the end-to-end distances do not only increase along the stretching axis but they should also decrease along the perpendicular axes to preserve the volume of the sample. A PLL chain constituted of 20 L-lysine residues, noted PLL20, was selected as simple model for our simulations. The MD simulations were performed in water with 20% of lysine residues charged along the polymer and chloride ions as counteranions of PLL20 to ensure the electrostatic neutrality of the system. First, we performed simulations with a nonconstrained PLL20 (i.e., the end-to-end distance from the α−carbon of the first lysine residue to the α−carbon of the last lysine residue can vary freely). The distance fluctuates between roughly 1.5 and 6 nm with an average value of 4.5 ± 0.8 nm (Figure S4A). It must however be noticed that most of the free-chain configurations correspond to end-to-end distances larger than 4.0 nm (76%). Yet, preliminary simulations showed that above 4.0 nm the PLL20 chains cannot adopt helical conformations because the PLL20 backbone is too elongated. Thus, we performed simulations of constrained systems where the end-to-end distance was fixed at successive values ranging from 2 up to 4 nm. This is also justified by the fact that experimentally smaller distances will become accessible while stretching (and not only larger ones). All the simulations were followed over 0.5 to 1 μs. Analysis of the secondary structures along the PLL20 as a function of time (Figure S4B) shows the absence of structure for the nonconstrained systems whereas as soon as the end-to-end distance ($d_{E\text{-}E}$) of the PLL20 chain becomes constrained to distances below 4.0 nm, the chains adopt transiently helical conformations (Figure S5A−F). Interestingly, not only the α-type helices is observed but also 3_{10}-helices were obtained. As example, snapshots of three typical observed conformations are given in Figure 6. Figure 7 shows the evolution of the helical content of the PLL20 chains as a function of the end-to-end distance for different simulations. A maximum of helicity was observed for an end-to-end distance of about 3.6 nm with the presence of α-helices and 3_{10}-helices.

Although the simulations were performed on small PLL chains (20 amino acids) they can guide a possible explanation

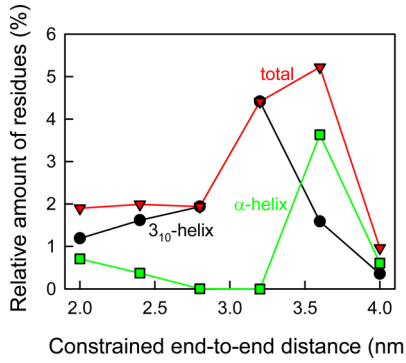

Figure 7. Helical content of the PLL20 chains as a function of the end-to-end distance as predicted by molecular dynamics simulations.

of our experimental findings, namely the appearance of helical configurations and in particular of 3_{10}-helices when stretching the cross-linked PLL/HA film. In summary, MD shows that in the nonconstrained state (free chains) the PLL20 chains do not adopt helical structures whereas when the end-to-end distance is fixed to values smaller than 4.0 nm, the chains adopt helix conformations. The absence of helicity for free PLL20 chains can be explained by the fact that configurations corresponding to end-to-end distances smaller than 4.0 nm are rare for free chains. In addition, even for configurations with small end-to-end distances, helical conformations represent only a small proportion of all conformations.

FRAP experiments have shown that cross-linking is equivalent to freeze the chains within the film (Figure S1) with a given end-to-end distance distribution. However, CD measurements further prove that this distribution does not induce the coil-to-helix transition. While stretching, the end-to-end distances do not only increase along the stretching axis but they should also decrease along the perpendicular axes. Now, our simulations show that helices appear in chains constrained to end-to-end distances smaller than the most frequent distances in free chains. This suggests that experimentally the distance reduction associated with stretching may cause the formation of helical conformations and in particular of 3_{10}-helices, never observed in solution. Finally it must be kept in mind that the simulations do not take the presence of HA chains into account. Now, stretching the film might also change the PLL-HA interaction which, in turn, could lead to such 3_{10}-helix formation. Taking into account the contribution of HA in

DOI: 10.1021/acsami.5b08302
ACS Appl. Mater. Interfaces 2016, 8, 14958−14965

MD simulations will require a high cost of calculation and thus this will be the purpose of a future study.

CONCLUSION

In summary, we have shown that stretching cross-linked PLL/HA films induces the formation of helices of the PLL chains. Our results suggest but do not prove that not only α- but also 3_{10}-helices form in the film under stretching. Such 3_{10}-helices have never been observed for PLL so far. The stretch-induced helix formation process is reversible, i.e. while returning to the nonstretched state one recovers the initial film structure. Using molecular dynamics simulations of PLL chains, we find that the unconstrained PLL20 chain never adopt a helical conformation. In contrast, when fixing the end-to-end distance of the PLL20 chain to distances smaller than the mean end-to-end distance of the free chain, a distance domain rarely explored by the free chain, helical conformations become accessible. Moreover, not only α- but also 3_{10}-helices are predicted by the simulations. These results suggest that the change of the end-to-end distance of PLL chains in the stretched film is at the origin of the helix formation.

Stretch-induced conformational changes in films constitute the basic process on which relies soft mechanochemistry. This study represents an important step toward the development of mechanocatalytic substrates where the catalytic activity of proteins or artificial enzymes embedded in the film can be controlled mechanically. Systems based on soft-mechanochemistry should find applications in catalysis where they offer the possibility of a mechanical control of the reaction kinetics. They should also be of interest in the biomedical field to design new types of biomaterials releasing drugs under mechanical forces applied by natural processes like vasodilatation or muscle contraction.

ASSOCIATED CONTENT

Supporting Information

The Supporting Information is available free of charge on the ACS Publications website at DOI: 10.1021/acsami.5b08302.

FRAP experiments on non-cross-linked and cross-linked PLL/HA films (Figure S1); CD spectra of non-cross-linked and cross-linked PLL/HA films in the non-stretched state (Figure S2); CD spectra of cross-linked films in the initial state and back to the nonstretched state after strains of 20, 40, and 60% (Figure S3); simulated end-to-end distance of a free PLL20 chain as a function of time (Figure S4A) and corresponding secondary structures (Figure S4B); simulated secondary structures of constrained PLL20 chains as a function of time (Figure S5A-F); details concerning the skewness of the CD spectra as a function of the weighted average of the wavelength within the domain 200−240 nm (Figure 4) (PDF)

AUTHOR INFORMATION

Corresponding Authors

*E-mail: schaaf@unistra.fr.

*E-mail: philippe.lavalle@inserm.fr.

Author Contributions

The authors declare no competing financial interests. The manuscript was written through contributions of all authors. All authors have given approval to the final version of the manuscript.

Funding

This work has been partially supported by icFRC (project "PSC-005"), USIAS, IUF, and from the European Union's Seventh Framework Program for research, technological development and demonstration under Grant Agreement No. 602694 (IMMODGEL).

Notes

The authors declare no competing financial interest.

ACKNOWLEDGMENTS

S.Z. acknowledges the Ministère de l'Enseignement Supérieur et de la Recherche for financial support.

ABBREVIATIONS

CD, circular dichroism
EDC, (N-ethyl-N′(3-(dimethylamino)propyl)carbodiimide hydrochloride
HA, hyaluronic acid
M, molar
NHS, *N*-hydroxysuccinimde)
PDMS, polydimethylsiloxane
PLL, poly(L-lysine)
PEI, poly(ethylenimine)
Tris, tris(hydroxymethyl)aminomethane
MD, molecular dynamics

REFERENCES

(1) Engler, A. J.; Griffin, M. A.; Sen, S.; Bonnemann, C. G.; Sweeney, H. L.; Discher, D. E. Myotubes Differentiate Optimally on Substrates with Tissue-Like Stiffness: Pathological Implications for Soft or Stiff Microenvironments. *J. Cell Biol.* **2004**, *166*, 877−887.

(2) Discher, D. E.; Janmey, P.; Wang, Y. L. Tissue Cells Feel and Respond to the Stiffness of Their Substrate. *Science* **2005**, *310*, 1139−1143.

(3) Li, B. J.; Moshfegh, C.; Lin, Z.; Albuschies, J.; Vogel, V. Mesenchymal Stem Cells Exploit Extracellular Matrix as Mechanotransducer. *Sci. Rep.* **2013**, *3*, No. #2425, DOI: 10.1038/srep02425.

(4) Mertz, D.; Vogt, C.; Hemmerlé, J.; Mutterer, J.; Ball, V.; Voegel, J. C.; Schaaf, P.; Lavalle, P. Mechanotransductive Surfaces for Reversible Biocatalysis Activation. *Nat. Mater.* **2009**, *8*, 731−735.

(5) Rios, C.; Longo, J.; Zahouani, S.; Garnier, T.; Vogt, C.; Reisch, A.; Senger, B.; Boulmedais, F.; Hemmerlé, J.; Benmlih, K.; Frisch, B.; Schaaf, P.; Jierry, L.; Lavalle, P. A New Biomimetic Route to Engineer Enzymatically Active Mechano-Responsive Materials. *Chem. Commun.* **2015**, *51*, 5622−5625.

(6) Ariga, K.; Mori, T.; Hill, J. P. Mechanical Control of Nanomaterials and Nanosystems. *Adv. Mater.* **2012**, *24*, 158−176.

(7) Onuchic, J. N.; Wolynes, P. G. Theory of Protein Folding. *Curr. Opin. Struct. Biol.* **2004**, *14*, 70−75.

(8) Ariga, K.; Yamauchi, Y.; Rydzek, G.; Ji, Q. M.; Yonamine, Y.; Wu, K. C. W.; Hill, J. P. Layer-by-Layer Nanoarchitectonics: Invention, Innovation, and Evolution. *Chem. Lett.* **2014**, *43*, 36−68.

(9) Buhot, A.; Halperin, A. Extension of Rod-Coil Multiblock Copolymers and the Effect of the Helix-Coil Transition. *Phys. Rev. Lett.* **2000**, *84*, 2160−2163.

(10) Tamashiro, M. N.; Pincus, P. Helix-Coil Transition in Homopolypeptides under Stretching. *Phys. Rev. E: Stat. Phys., Plasmas, Fluids, Relat. Interdiscip. Top.* **2001**, *63*, No. #021909, DOI: 10.1103/PhysRevE.63.021909.

(11) Courty, S.; Gornall, J. L.; Terentjev, E. M. Mechanically Induced Helix-Coil Transition in Biopolymer Networks. *Biophys. J.* **2006**, *90*, 1019−1027.

(12) Torabi, K.; Schatz, G. C. Tensile Mechanics of Alpha-Helical Polypeptides. *Macromolecules* **2013**, *46*, 7947−7956.

(13) Seol, Y.; Skinner, G. M.; Visscher, K.; Buhot, A.; Halperin, A. Stretching of Homopolymeric RNA Reveals Single-Stranded Helices

DOI: 10.1021/acsami.5b08302
ACS Appl. Mater. Interfaces 2016, 8, 14958−14965

and Base-Stacking. *Phys. Rev. Lett.* **2007**, *98*, No. #158103, DOI: 10.1103/PhysRevLett.98.158103.
(14) Courty, S.; Gornall, J. L.; Terentjev, E. M. Induced Helicity in Biopolymer Networks under Stress. *Proc. Natl. Acad. Sci. U. S. A.* **2005**, *102*, 13457−13460.
(15) Tang, Z. Y.; Wang, Y.; Podsiadlo, P.; Kotov, N. A. Biomedical Applications of Layer-by-Layer Assembly: From Biomimetics to Tissue Engineering. *Adv. Mater.* **2006**, *18*, 3203−3224.
(16) Cohen Stuart, M. A.; Huck, W. T. S.; Genzer, J.; Muller, M.; Ober, C.; Stamm, M.; Sukhorukov, G. B.; Szleifer, I.; Tsukruk, V. V.; Urban, M.; Winnik, F.; Zauscher, S.; Luzinov, I.; Minko, S. Emerging Applications of Stimuli-Responsive Polymer Materials. *Nat. Mater.* **2010**, *9*, 101−113.
(17) Boudou, T.; Crouzier, T.; Ren, K. F.; Blin, G.; Picart, C. Multiple Functionalities of Polyelectrolyte Multilayer Films: New Biomedical Applications. *Adv. Mater.* **2010**, *22*, 441−467.
(18) Hammond, P. T. Building Biomedical Materials Layer-by-Layer. *Mater. Today* **2012**, *15*, 196−206.
(19) Schneider, A.; Francius, G.; Obeid, R.; Schwinté, P.; Hemmerlé, J.; Frisch, B.; Schaaf, P.; Voegel, J.-C.; Senger, B.; Picart, C. Polyelectrolyte Multilayers with a Tunable Young's Modulus: Influence of Film Stiffness on Cell Adhesion. *Langmuir* **2006**, *22*, 1193−1200.
(20) Pavlukhina, S.; Lu, Y. M.; Patimetha, A.; Libera, M.; Sukhishvili, S. Polymer Multilayers with pH-Triggered Release of Antibacterial Agents. *Biomacromolecules* **2010**, *11*, 3448−3456.
(21) Decher, G. Fuzzy nanoassemblies: Toward Layered Polymeric Multicomposites. *Science* **1997**, *277*, 1232−1237.
(22) Lavalle, P.; Gergely, C.; Cuisinier, F. J. G.; Decher, G.; Schaaf, P.; Voegel, J. C.; Picart, C. Comparison of the Structure of Polyelectrolyte Multilayer Films Exhibiting a Linear and an Exponential Growth Regime: An in Situ Atomic Force Microscopy Study. *Macromolecules* **2002**, *35*, 4458−4465.
(23) Townend, R.; Kumosinski, T. F.; Timasheff, S. N.; Fasman, G. D.; Davidson, B. The Circular Dichroism of the Beta Structure of Poly-L-Lysine. *Biochem. Biophys. Res. Commun.* **1966**, *23*, 163−169.
(24) Mirtic, A.; Grdadolnik, J. The Structure of Poly-L-Lysine in Different Solvents. *Biophys. Chem.* **2013**, *175*, 47−53.
(25) Picart, C.; Mutterer, J.; Richert, L.; Luo, Y.; Prestwich, G. D.; Schaaf, P.; Voegel, J.-C.; Lavalle, P. Molecular Basis for the Explanation of the Exponential Growth of Polyelectrolyte Multilayers. *Proc. Natl. Acad. Sci. U. S. A.* **2002**, *99*, 12531−12535.
(26) Picart, C.; Sengupta, K.; Schilling, J.; Maurstad, G.; Ladam, G.; Bausch, A. R.; Sackmann, E. Microinterferometric Study of the Structure, Interfacial Potential, and Viscoelastic Properties of Polyelectrolyte Multilayer Films on a Planar Substrate. *J. Phys. Chem. B* **2004**, *108*, 7196−7205.
(27) Picart, C.; Senger, B.; Sengupta, K.; Dubreuil, F.; Fery, A. Measuring Mechanical Properties of Polyelectrolyte Multilayer Thin Films: Novel Methods Based on AFM and Optical Techniques. *Colloids Surf., A* **2007**, *303*, 30−36.
(28) Vogt, C.; Ball, V.; Mutterer, J.; Schaaf, P.; Voegel, J. C.; Senger, B.; Lavalle, P. Mobility of Proteins in Highly Hydrated Polyelectrolyte Multilayer films. *J. Phys. Chem. B* **2012**, *116*, 5269−5278.
(29) Schneider, C. A.; Rasband, W. S.; Eliceiri, K. W. NIH Image to ImageJ: 25 Years of Image Analysis. *Nat. Methods* **2012**, *9*, 671−675.
(30) Goetz, A. W.; Williamson, M. J.; Xu, D.; Poole, D.; Le Grand, S.; Walker, R. C. Routine Microsecond Molecular Dynamics Simulations with AMBER on GPUs. 1. Generalized Born. *J. Chem. Theory Comput.* **2012**, *8*, 1542−1555.
(31) Hornak, V.; Abel, R.; Okur, A.; Strockbine, B.; Roitberg, A.; Simmerling, C. Comparison of Multiple Amber Force Fields and Development of Improved Protein Backbone Parameters. *Proteins: Struct., Funct., Genet.* **2006**, *65*, 712−725.
(32) Maier, J. A.; Martinez, C.; Kasavajhala, K.; Wickstrom, L.; Hauser, K. E.; Simmerling, C. ff14SB: Improving the Accuracy of Protein Side Chain and Backbone Parameters from ff99SB. *J. Chem. Theory Comput.* **2015**, *11*, 3696−3713.
(33) Joung, I. S.; Cheatham, T. E., 3rd Determination of Alkali and Halide Monovalent Ion Parameters for Use in Explicitly Solvated Biomolecular Simulations. *J. Phys. Chem. B* **2008**, *112*, 9020−9041.
(34) Joung, I. S.; Cheatham, T. E., 3rd Molecular Dynamics Simulations of the Dynamic and Energetic Properties of Alkali and Halide Ions Using Water-Model-Specific Ion Parameters. *J. Phys. Chem. B* **2009**, *113*, 13279−13290.
(35) Jorgensen, W. L.; Chandrasekhar, J.; Madura, J. D.; Impey, R. W.; Klein, M. L. Comparison of Simple Potential Functions for Simulating Liquid Water. *J. Chem. Phys.* **1983**, *79*, 926−935.
(36) Roe, D. R.; Cheatham, T. E. PTRAJ and CPPTRAJ: Software for Processing and Analysis of Molecular Dynamics Trajectory Data. *J. Chem. Theory Comput.* **2013**, *9*, 3084−3095.
(37) Humphrey, W.; Dalke, A.; Schulten, K. VMD: Visual Molecular Dynamics. *J. Mol. Graphics* **1996**, *14*, 33−38.
(38) Drake, A. F.; Siligardi, G.; Gibbons, W. A. Reassessment of the Electronic Circular-Dichroism Criteria for Random Coil Conformations of Poly(L-Lysine) and the Implications for Protein Folding and Denaturation Studies. *Biophys. Chem.* **1988**, *31*, 143−146.
(39) Sreerama, N.; Woody, R. W. Poly(Pro)II Helices in Globular-Proteins - Identification and Circular Dichroic Analysis. *Biochemistry* **1994**, *33*, 10022−10025.
(40) Greenfield, N.; Fasman, G. D. Computed Circular Dichroism Spectra for the Evaluation of Protein Conformation. *Biochemistry* **1969**, *8*, 4108−4116.
(41) Di Mauro, A.; Mirabella, F.; D'Urso, A.; Randazzo, R.; Purrello, R.; Fragala, M. E. Spontaneous Deposition of Polylysine on Surfaces: Role of the Secondary Structure to Optimize Noncovalent Coating Strategies. *J. Colloid Interface Sci.* **2015**, *437*, 270−276.
(42) Toniolo, C.; Polese, A.; Formaggio, F.; Crisma, M.; Kamphuis, J. Circular Dichroism Spectrum of a Peptide 3(10)-Helix. *J. Am. Chem. Soc.* **1996**, *118*, 2744−2745.
(43) Toniolo, C.; Benedetti, E. The Polypeptide-3(10)-Helix. *Trends Biochem. Sci.* **1991**, *16*, 350−353.
(44) De Zotti, M.; Biondi, B.; Peggion, C.; Formaggio, F.; Park, Y.; Hahm, K. S.; Toniolo, C. Trichogin GA IV: A Versatile Template for the Synthesis of Novel Peptaibiotics. *Org. Biomol. Chem.* **2012**, *10*, 1285−1299.

DOI: 10.1021/acsami.5b08302
ACS Appl. Mater. Interfaces 2016, 8, 14958−14965